Identical Pion Interferometry from Au+Au Collisions at $\sqrt{s_{\mathrm{NN}}}$ = 3, 3.2, 3.5, and 3.9 GeV in the STAR Experiment at RHIC

V.B. Luong[1] *(for the STAR Collaboration)*

Joint Institute for Nuclear Research

Two-pion interferometry provides access to the spatial and temporal size, shape, and evolution of the sources created in heavy ion collisions, offering strong constraints for theoretical models. In these proceedings, we will report the measurement of correlation strength (λ) and femtoscopic radii (R_{out}, R_{side}, R_{long}, $R^2_{\mathrm{out-long}}$) extracted from the two-pion correlation function in Au+Au collisions at $\sqrt{s_{\mathrm{NN}}}$ = 3, 3.2, 3.5, and 3.9 GeV. The dependences of these parameters on pair transverse momentum, pair rapidity, collision centrality, and collision energy will be presented, and their physics implications will be discussed.

PACS: 25.75.Gz, 25.75.Nq

INTRODUCTION

The correlation femtoscopy technique can be used to extract information about the space-time evolution of the particle-emitting sources in heavy ion collisions [1]. Hence, such measurements offer robust constraints for the models of heavy ion collisions. The Solenoidal Tracker At RHIC (STAR) experiment at the Relativistic Heavy Ion Collider (RHIC) has studied pion femtoscopic correlations in Au+Au collisions over a broad energy range during the Beam Energy Scan (BES) I program [2]. In the BES-II program, the Fixed-Target (FXT) mode [3] at STAR has extented the feasible collision energies at RHIC below $\sqrt{s_{\mathrm{NN}}}$ = 7.7 GeV.

In these proceedings, we present the preliminary results of femtoscopic measurements of pairs of identical pions in Au+Au collisions at $\sqrt{s_{\mathrm{NN}}}$ = 3, 3.2, 3.5, and 3.9 GeV, which were collected by the STAR experiment during the FXT program.

[1]E-mail: vinhbluong@jinr.ru

ANALYSIS METHOD

Experimentally, the two-particle correlation functions can be measured by the following ratio:

$$C(\mathbf{q}) = \frac{N(\mathbf{q})}{D(\mathbf{q})} \tag{1}$$

where $\mathbf{q} \equiv \mathbf{p}_1 - \mathbf{p}_2$ is the relative momenta of the first ($\mathbf{p}_1$) and the second ($\mathbf{p}_2$) particles from a pair . The numerator distribution ($N(\mathbf{q})$) is constructed from pairs in which both constituent tracks are from the same event, while the denominator distribution ($D(\mathbf{q})$) is constructed from pairs formed from tracks coming from different events. For the case of pion correlation femtoscopy, while both $N(\mathbf{q})$ and $D(\mathbf{q})$ encapsulate two-particle phase-space information, the $N(\mathbf{q})$ contains additional contributions from Bose-Einstein correlations and Coulomb interactions.

To mitigate the two-track detector effects on measured correlation functions, specific pair selection criteria are implemented. The two-track detector effects are track splitting, when one track is reconstructed as two distinct tracks, and track merging, when only one track is reconstructed out of two closely emitted particles. These pair selection criteria are applied equally for both $N(\mathbf{q})$ and $D(\mathbf{q})$.

Particles forming the pair are boosted to the longitudinal comoving system (LCMS), where the longitudinal components of their momenta cancel each other, $p_{z,1} + p_{z,2} = 0$. The pair relative momentum is then decomposed into Bertsch-Pratt [4, 5] "out-side-long" coordinate system. In this system, the "out" direction (q_{out}) lies along the pair transverse momentum, $\mathbf{k}_{\text{T}} \equiv (\mathbf{p}_{\text{T},1} + \mathbf{p}_{\text{T},2})/2$, "long" direction ($q_{\text{long}}$) is parallel to the beam axis, and "side" direction (q_{side}) is perpendicular to the other two.

The Bowler-Sinyukov [6, 7] procedure is used to fit and extract the femtoscopic parameters:

$$C(\mathbf{q}) = N\left[(1-\lambda) + \lambda K_{\text{Coul}}(q_{\text{inv}}) G(\mathbf{q})\right] \tag{2}$$

where

$$G(\mathbf{q}) = 1 + \exp(-q_{\text{out}}^2 R_{\text{out}}^2 - q_{\text{side}}^2 R_{\text{side}}^2 - q_{\text{long}}^2 R_{\text{long}}^2 - 2 q_{\text{out}} q_{\text{long}} R_{\text{out-long}}^2) \tag{3}$$

is the quantum-statistical part of the correlation function, assuming a Gaussian form of the particle-emitting sources. N is the normalization factor, λ is the correlation strenth, K_{Coul} is the Coulomb correction factor. Femtoscopic radii: R_{out}, R_{side}, R_{long} give the length of homogeneity regions in the "out", "side", and "long" directions, respectively. $R_{\text{out-long}}^2$ is the off-diagonal element describing the twist of the two-dimentional correlation functions in the "out-long" plane. For a symmetric acceptance w.r.t. midrapidity and azimuthal-integrated femtoscopy analysis, the correlation functions are symmetric w.r.t q_{out} and q_{long} axes, hence, $R_{\text{out-long}}^2$ should be consistent with zero. This usually applies for collider experiments.

RESULTS AND DISCUSSIONS

The results of the fitting procedure is demonstrated in Fig. 1 for midrapidity pions with $-0.5 < y_{\rm single} < 0$ and $0.15 < k_{\rm T} < 0.25$ GeV/c from 0-10% central Au+Au collisions. The upper row of Fig. 1 shows the projections of the correlation functions onto $q_{\rm out}$, $q_{\rm side}$, $q_{\rm long}$ axes. For each projection, the other components of $\mathbf{q}$ are integrated over the range of ± 35 MeV/c. The lower row of Fig. 1 depicts the comparison of correlation functions between positively and negatively charged pion pairs. A difference of a few percentage is observed in the correlation functions between positively and negatively charged pion pairs.

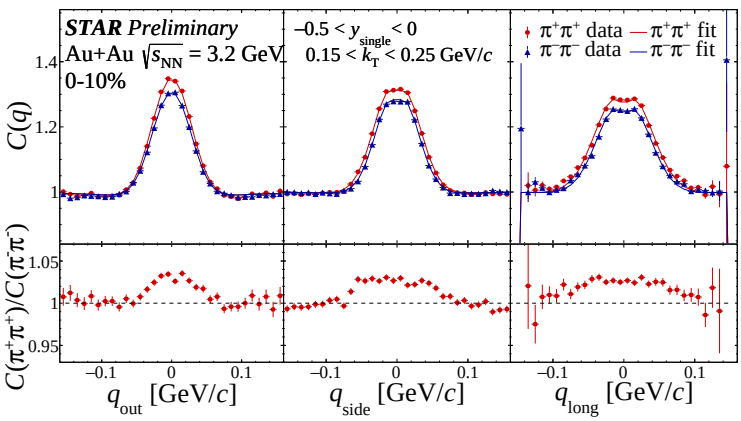

Fig. 1. Top row: Projections of the correlation functions in the LCMS frame onto the $q_{\rm out}$, $q_{\rm side}$, and $q_{\rm long}$ axes for $\pi^+\pi^+$ (circles) and $\pi^-\pi^-$ (triangles) pairs for $0.15 < k_{\rm T} < 0.25$ GeV/c from 0-10% central Au+Au collisions at $\sqrt{s_{\rm NN}} = 3.2$ GeV. The curves show the projections of the 3-dimentional fit to the correlation functions. Bottom row: The ratio of the correlation functions between $\pi^+\pi^+$ and $\pi^-\pi^-$ pairs. Errors are statistical only.

Fig. 2 shows the dependence of extracted femtoscopic parameters on the pair transverse momentum of pions with $-0.5 < y_{\rm single} < 0$ in Au+Au collisions at $\sqrt{s_{\rm NN}} = 3.2$ GeV. The $R_{\rm out}$, $R_{\rm side}$, $R_{\rm long}$ radii decrease from central to peripheral collisions reflecting changes in geometry of the overlapping area of the collisions. The decrease of radii as $k_{\rm T}$ increasing is also evident and can be attributed to the radial flow resulting from the hydrodynamical expansion of the emitting source. The extracted cross term $R^2_{\rm out-long}$ is non-zero across all collision centralities and $k_{\rm T}$ due to the asymmetrical acceptance with respect to midrapidity.

The collision energy dependence of femtoscopic parameters is presented in Fig. 3. To compare with other experiments, pions at midrapidity ($-0.5 < y_{\rm single} < 0$) and $0.15 < k_{\rm T} < 0.25$ GeV/c in 0-10% central Au+Au collisions are selected. The statistical and systematical uncertainties were added in quadrature. For discussions about variations in centrality, $k_{\rm T}$, and analysis techniques between published results, see Ref. [2, 8] and references therein. For STAR published results at $\sqrt{s_{\rm NN}} = 7.7$–200 GeV from Ref. [2], only

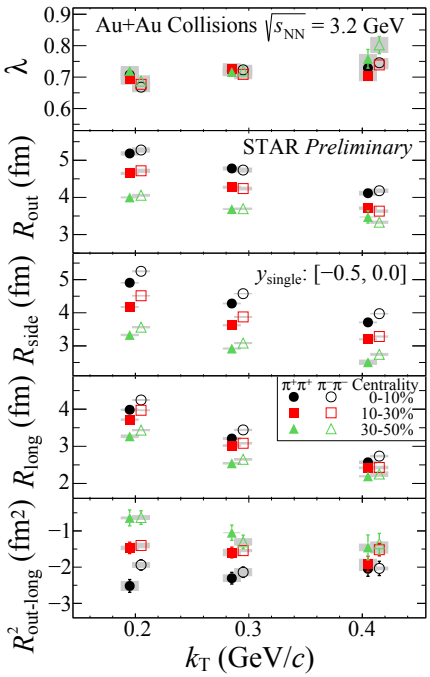

Fig. 2. Pair transverse momentum dependence of extracted femtoscopic parameters for 0-10% (circles), 10-30% (squares), 30-50% (triangles) centrality classes from Au+Au collisions at $\sqrt{s_{NN}} = 3.2$ GeV. Pairs are formed from pions with $-0.5 < y_{single} < 0$. Results for $\pi^-\pi^-$ and $\pi^+\pi^+$ are shown by open and closed markers, respectively. Shaded boxes denote systematic uncertainties.

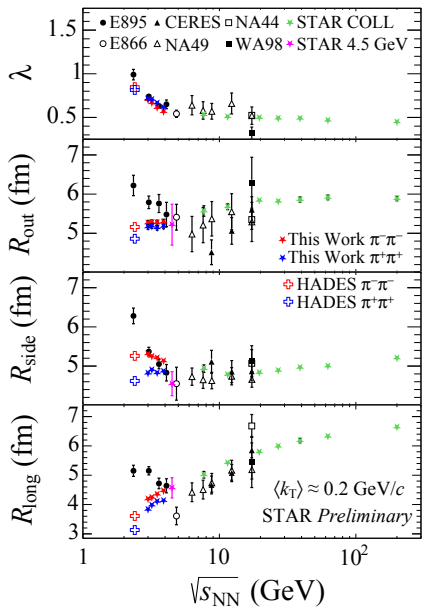

Fig. 3. Collision energy dependence of extracted femtoscopic parameters of midrapidity pions and $\langle k_T \rangle \approx 0.2$ GeV/c in Au+Au, Pb+Pb, and Pb+Au central collisions.

statistical uncertainty was plotted. The extracted pion femtoscopic radii of the current analysis favour the global trend established by HADES [8]

and previously published results by STAR at higher energies [2, 3]. A slight decrease of $R_{\rm side}$ and increase of $R_{\rm long}$ with increasing collision energy are observed as the emitting source evolves from oblate to prolate.

Fig. 4 depicts the acceptance of pion pairs at $\sqrt{s_{\rm NN}}$ = 3–3.9 GeV measured by the STAR experiment during the FXT program. The acceptance is plotted as two-dimensional distributions of pair transverse momentum and pair rapidity in the center-of-mass (CMS) frame, $y_{\rm pair}^{\rm CMS} \equiv y_{\rm c.m.} - y_{\rm pair}$. $y_{\rm c.m.}$ and $y_{\rm pair}$ are the midrapidity and pair rapidity in the laboratory frame, respectively. For each collision energy, five pair rapidity bins with $0.15 < k_{\rm T} < 0.6$ GeV/c were selected for the rapidity-differential analysis. It can be noted that the higher collision energy is, the futher $y_{\rm c.m.}$ is shifted away from the STAR central barrel, and the more asymetric the pair acceptance is w.r.t. midrapidity, $y_{\rm pair}^{\rm CMS} = 0$.

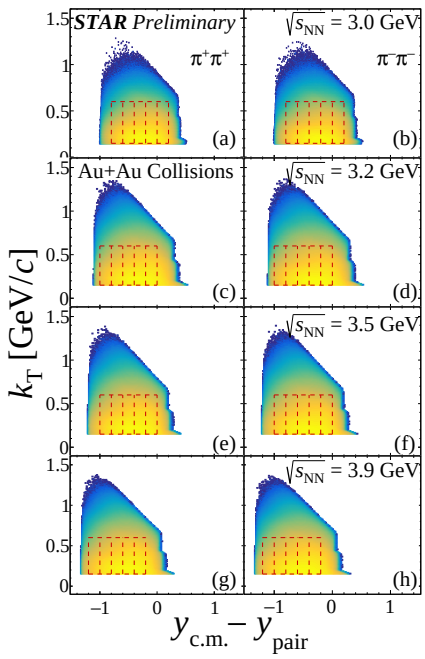

Fig. 4. Pair acceptance of positively (left column) and negatively (right column) charged for $\sqrt{s_{\rm NN}}$ = 3–3.9 GeV. Red rectangles denote selected windows for the rapidty-differential analysis.

Fig. 5 shows the pair rapidity dependence of extracted femtoscopic parameters of pion pairs at $\sqrt{s_{\rm NN}}$ = 3–3.9 GeV in the collision center-of-mass frame. The colored markers depict measured data points by STAR, and the gray markers are the mirrored data points w.r.t. midrapidity. The $R^2_{\rm out-long}$ clearly depends on pair rapidity, weakly depends on centrality, and is consistent between positively and negatively charged pairs. The observed pair rapidity dependence of $R_{\rm side}$, most pronounced in central collisions at $\sqrt{s_{\rm NN}} = 3$ GeV, suggests boost invariance breaking of the emitting pion source. The charge splitting is observed for $R_{\rm side}$ and $R_{\rm long}$, which is smaller at higher collision energy, and in less central collisions. This effect may be attributed to the Coulomb interactions between the emitting source and the fireball [8].

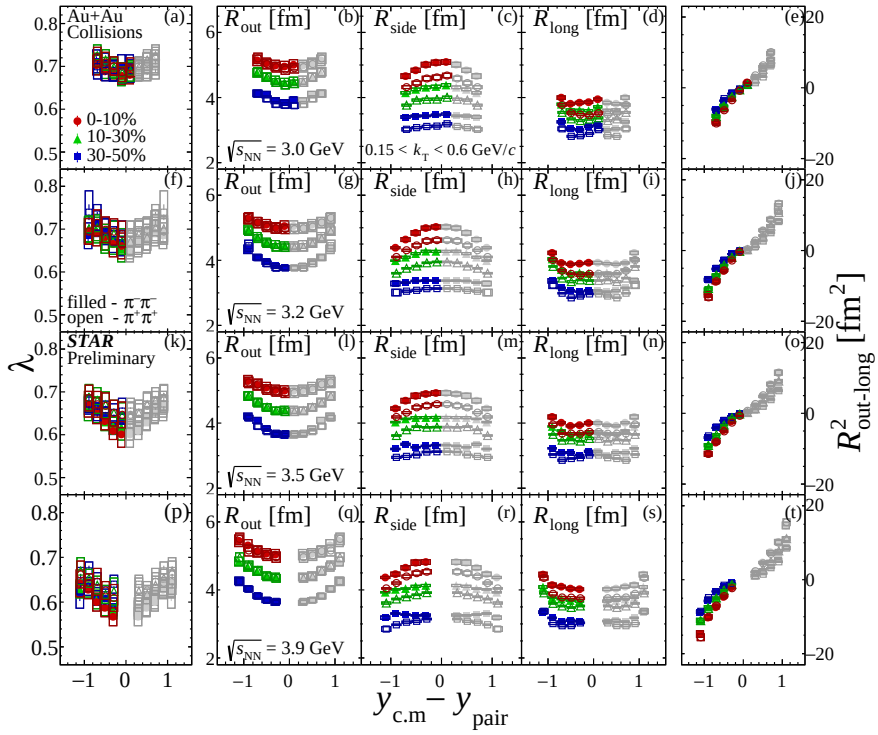

Fig. 5. Pair rapidity dependence of λ, $R_{\rm out}$, $R_{\rm side}$, $R_{\rm long}$, and $R^2_{\rm out-long}$ for 0-10% (circles), 10-30% (triangles), 30-50% (squares) centrality classes from Au+Au collisions at $\sqrt{s_{\rm NN}}$ = 3.0, 3.2, 3.5, and 3.9 GeV. The closed markers are for $\pi^-\pi^-$ and the open markers for $\pi^+\pi^+$ pairs. Gray markers are mirrored data points w.r.t. midrapidity. The systematic uncertainties are shown by boxes. The statistical uncertainties are smaller than the marker size.

CONCLUSION

In these proceedings, preliminary results of pion femtoscopic correlations in Au+Au collisions at $\sqrt{s_{\rm NN}}$ = 3, 3.2, 3.5, and 3.9 GeV from the STAR experiment are presented. The extracted femtoscopic parameters are studied as functions of centrality, pair transverse momentum, pair rapidity, and collision energy.

The apparent transverse momentum and centrality dependences of $R_{\rm out}$, $R_{\rm side}$, $R_{\rm long}$ can be attributed to radial flow and collision geometry, respectively. The collision energy dependence of femtoscopic radii favour the trend formed by results from HADES and STAR at higher energies. A slight decrease of $R_{\rm side}$ and increase of $R_{\rm long}$ with increasing collision energy are observed as the emitting source evolves from oblate to prolate. Furthermore, we note a difference in the correlation function and, subsequently, in the extracted $R_{\rm side}$, $R_{\rm long}$ between positively and negatively charged pion pairs. This charge splitting could be due to the Coulomb interactions between the emitting source and the fireball. Finally, the observed dependence of $R_{\rm side}$ on pair rapidity implies the boost-invariance breaking of the emitting sources.

REFERENCES

1. *Lisa M.A., Pratt S., Soltz R., Wiedemann U.* Femtoscopy in relativistic heavy ion collisions // Ann. Rev. Nucl. Part. Sci.. — 2005. — V. 55. — P. 357–402. — arXiv:nucl-ex/0505014 [nucl-ex].

2. *Adamczyk L. et al.* [STAR Collaboration] Beam-energy-dependent two-pion interferometry and the freeze-out eccentricity of pions measured in heavy ion collisions at the STAR detector // Phys. Rev. C. — 2015. — V. 92, no. 1. — P. 014904. — arXiv:1403.4972 [nucl-ex].

3. *Adam J. et al.* [STAR Collaboration] Flow and interferometry results from Au+Au collisions at $\sqrt{s_{\rm NN}} = 4.5$ GeV // Phys. Rev. C. — 2021. — V. 103, no. 3. — P. 034908. — arXiv:2007.14005 [nucl-ex].

4. *Pratt S.* Pion Interferometry of Quark-Gluon Plasma // Phys. Rev. D — 1986. — V. 33. — P. 1314–1327.

5. *Bertsch G., Gong M., Tohyama M.* Pion Interferometry in Ultrarelativistic Heavy Ion Collisions // Phys. Rev. C — 1988. — V. 37. — P. 1896–1900.

6. *Bowler M.G.* Coulomb corrections to Bose-Einstein correlations have been greatly exaggerated // Phys. Lett. B — 1991. — V. 270. — P. 69–74.

7. *Sinyukov Y., Lednicky R., Akkelin S.V., Pluta J., Erazmus B.* Coulomb corrections for interferometry analysis of expanding hadron systems // Phys. Lett. B — 1998. — V. 432. — P. 248–257.

8. *Adamczewski-Musch J. et al.* [HADES Collaboration] Identical pion intensity interferometry in central Au+Au collisions at 1.23 AGeV // Phys. Lett. B. — 2019. — V. 795. — P. 446–451. — arXiv:1811.06213 [nucl-ex].